ELSEVIER

Catalysis Today 67 (2001) 127–138

CATALYSIS TODAY

www.elsevier.com/locate/cattod

# Use of zeolite membrane reactors for selectivity enhancement: application to the liquid-phase oligomerization of *i*-butene

Elena Piera, Carlos Téllez, Joaquín Coronas, Miguel Menéndez, Jesús SaIntamaría*

*Department of Chemical and Environmental Engineering, Faculty of Science, University of Zaragoza, 50009 Zaragoza, Spain*

**Abstract**

This work investigates the use of a zeolite membrane reactor (ZMR) in the liquid-phase oligomerization of *i*-butene. The membrane was used for the selective removal of *i*-octene from the reaction environment, thus reducing the formation of unwanted $C_{12}$ and $C_{16}$ hydrocarbons. MFI (silicalite) membranes prepared by secondary growth on stainless steel porous tubes were used for this purpose, given the non-polar nature of the compounds to be separated. Preliminary non-reactive tests demonstrated the capability of the membrane to separate *i*-octene from *i*-butene and from $C_{12}$ and $C_{16}$ hydrocarbons. Reaction experiments were then carried out over an acid resin catalyst bed located on the membrane tube side. The ZMR produced a very significant increase in the selectivity, and as a consequence also in the yield of *i*-octenes (intermediate product in the oligomerization of *i*-butene), compared to a conventional fixed bed reactor (FBR). 

*Keywords:* Oligomerization; Selectivity increase; Zeolite membrane reactor

## 1. Introduction

Different membrane reactor configurations have been proposed in selectivity-enhancing applications. The most commonly used involves the distribution of a reactant in series-parallel reacting networks when there is a favorable kinetic effect regarding the partial pressure of the distributed species. This is frequently the case with selective oxidation processes, where a low partial pressure of oxygen favors the selective oxidation reaction versus the combustion to CO and $CO_2$. Since oxygen is a necessary reactant, its presence in the reaction environment cannot be completely avoided, but its partial pressure in the vicinity of the catalytic particles can be lowered by distributing it along the bed. In inert membrane reactors this is achieved by distributing oxygen to the catalyst bed using a porous membrane (e.g. [1,2]), while in catalytic membrane reactors the partial pressure of oxygen is lowered by using a diffusion layer coupled to the catalytic layer of the membrane (e.g. [3]).

Microporous membranes provide additional opportunities to increase the reaction selectivity. Thus, selectivity improvements have been reported with microporous catalytic membranes operating with single-file diffusion in the flow-through mode. In this case consecutive reactions are limited to adjacent molecules, and a careful dosing of reactants allows to increase the selectivity by suppressing overreaction [4]. Another possibility, with which this work is concerned, consists of removing a valuable intermediate product before it reacts further in consecutive reaction networks. In this case, a considerable increase in the yield to the desired product can be obtained, provided that the membrane is sufficiently selective to the intermediate product under reaction conditions.

* Corresponding author. Tel.: +34-976-76-1153; fax: +34-976-76-2142.
*E-mail address:* iqcatal@posta.unizar.es (J. SaIntamaría).

0920-5861/01/$ – see front matter 
PII: S0920-5861(01)00304-2

**Nomenclature**

| | |
|---|---|
| $m_i$ | molar flowrate of component $i$ (mol $s^{-1}$) |
| $P_p$ | permeate pressure (Pa) |
| $P_r$ | retentate pressure (Pa) |
| $PF_i$ | permeation flux of component $i$ (mol $m^{-2}$ $s^{-1}$) |
| $r$ | inner radius of the membrane |
| $R_i$ | reaction rate of component $i$ (mol $kg^{-1}$ of catalyst per s) |
| $S_i$ | reaction selectivity of component $i$ |
| $x_i$ | molar fraction of component $i$ in the retentate |
| $X_{i\text{-butene}}$ | $i$-butene conversion |
| $y_i$ | molar fraction of component $i$ in the permeate |
| $z$ | length of catalysts bed (m) |

*Greek letters*

| | |
|---|---|
| $\alpha_{C_8/i}$ | separation factor of $C_8$ with respect to component $i$ |
| $\nu_i$ | carbon number of species $i$ |
| $\rho_L$ | catalyst density in the bed (kg $m^{-3}$) |

The specific characteristics of zeolite membranes make them ideal candidates to integrate reaction and separation [5]. In spite of this, applications of this type in the open literature are still scarce. Among the few examples are the dehydrogenation of *i*-butane to *i*-butene [6]; the methatesis of propene to ethylene and 2-butene, and of 2-butene to *cis*- and *trans*-2-butene [7] and the synthesis of MTBE [8]. These works used zeolite membranes to increase conversion by selective product removal in equilibrium-limited systems. An increase of conversion in the Fischer–Tropsch process by selective water removal with zeolite membranes has also been reported, but in this case the reasons for the conversion increase are different: the presence of water decreases the reaction rate and causes catalyst deactivation [9]. The present work is concerned with the use of zeolite membrane reactors (ZMRs) to increase the selectivity by preferential removal of a reactive intermediate product, more specifically, *i*-octene, produced during the oligomerization of *i*-butene. The motivation for this work stems from the environmental problems associated to MTBE: due to groundwater pollution, MTBE is being questioned as a component of reformulated gasoline [10], and its use will be phased out in California by the end of 2002. Other states and countries are facing similar problems, and it seems likely that MTBE production will suffer a steep decline in the near future. The dimerization of *i*-butene into branched octenes is now regarded as one of the main alternatives for the production of high-octane gasoline. This exothermic process, that is usually carried out in liquid-phase, produces not only *i*-octenes, but also undesired $C_{12}$ or even $C_{16}$ species, giving rise to a reaction selectivity problem. It would be highly desirable to remove the $C_8$ intermediate product from the reaction atmosphere, before it reacts further to give $C_{12}$ and $C_{16}$ products. This could in principle be achieved with membrane reactors in which the membrane would provide selective transport of the $C_8$ components as these are produced, thereby removing them from the reaction atmosphere and increasing the $C_8$ yield.

In this case, a catalyst bed of acid-resin (Amberlyst$^{TM}$ 15) was packed on the tube side of a tubular membrane to conform an inert ZMR, whose performance at several conditions was evaluated and compared to that of a fixed bed reactor (FBR). Also, from the results of the FBR experiments, power-law kinetics were obtained and used to build a simple mathematical model used for simulation of the ZMR.

## 2. Experimental

MFI (silicalite) membranes were prepared by secondary growth on stainless steel porous tubes. To this end a two step synthesis procedure has been used following the directions given elsewhere [11]: first, silicalite crystal seeds were prepared under hydrothermal synthesis conditions in a teflon-lined autoclave. Then, the porous stainless steel tubular supports (from Mott, with 500 nm pore diameter, inner/outer diameters 0.635/0.953 cm) were dip-coated 10 times with silicalite seeds, and the seeded supports were then subjected to hydrothermal synthesis. The synthesis gel used to prepare the crystal seeds had the following molar composition [12]: $110H_2O$:$10SiO_2$:1NaOH: 2.4TPAOH, where TPAOH is tetrapropylammonium hydroxide and the silica source was Aerosil 300. This gel was heated at 130°C for 2 h in a teflon-lined

autoclave. The suspension obtained was centrifuged and washed with deionized water several times until pH = 7 was obtained. A seed suspension was then prepared by adjusting the water content to give a concentration of crystal seeds of 20 g $l^{-1}$. For the secondary growth of the silicalite membranes two different gels were used. Gel A [12] had the following molar composition: 1TPABr:20TEOS:560$H_2O$:0.9KOH, where TPABr is tetrapropylammonium bromide and TEOS is tetra-ethyl-*ortho*-silicate; the composition of gel B [13]. was: 1TPABr:21$SiO_2$:788$H_2O$:3NaOH, in this case, the silica source was Aerosil 300. Before the introduction of the support in the autoclave, one end of the wet tube was wrapped with Teflon tape, plugged with a teflon cap and filled with the secondary growth gel, the other end was wrapped with tape and plugged with another teflon cap. The autoclave was placed vertically in a convection oven at 150–170°C for 8–15 h and the synthesis was repeated three to four times until an impermeable membrane was obtained. The template was then removed by heating up to 480°C with a heating rate of 1°C $min^{-1}$ followed by calcination at this temperature for 8 h.

$N_2$ and $SF_6$ single gas permeances were measured, and the $N_2/SF_6$ ideal selectivity was used as an indication of the quality of the membrane; in addition, the separation selectivity was measured in gas phase separation experiments with binary mixtures of 2,4,4-trimethyl-1-pentene and *i*-butene, and in pervaporation experiments with a liquid-phase feed containing a ternary mixture of 2,4,4-trimethyl-1-pentene, 1-dodece and 1-hexadecene. In the gas phase experiments, a stream of 25 Nml $min^{-1}$ of *i*-butene saturated at room temperature with *i*-octene was fed to the tube side (retentate) of the membrane, at *i*-octene partial pressures in the feed between 1.5 and 2.9 kPa. The permeate was swept with 9 Nml $min^{-1}$ of $N_2$. In the pervaporation experiments, 0.5 ml $min^{-1}$ of the ternary liquid-phase mixture were fed by means of a HPLC pump (Shimadzu LC-10ADvp) to the retentate side at pressures in the 3–25 bar range (usually at 15 bar), while the permeate side was kept at room pressure and swept with 43 Nml $min^{-1}$ of $N_2$. All the gas streams supplied to the membrane were mass-flow controlled (Brooks 5850).

Reaction experiments were carried out using an experimental system similar to that described previously [8], except that in this case the reaction was carried out in the liquid-phase. Briefly, an *i*-butene liquid stream was fed by means of a HPLC pump to the catalyst bed on the tube side of the membrane. The ZMR normally operated at 15 bar, with space velocities in the range of 2.5–105 $h^{-1}$ (kg *i*-butene/kg catalyst per h), at temperatures ranging from 20 to 85°C and with $N_2$ sweep gas flowrates from 150 to 1600 Nml $min^{-1}$. The temperature of the membrane reactor was controlled by immersing it in a thermostatic oil bath (Julabo F34-MD). The catalyst bed was a mixture of 0.35 g of Amberlyst$^{TM}$ 15 (mean particle size, 20–30 mesh) and 0.90 g of quartz (approximately same particle size), used as an inert diluent due to the exothermicity of the process. In both separation and reaction experiments, the membrane was sealed in a stainless steel membrane module by means of graphite gaskets. For the FBR experiments, the same amount of resin and quartz was used, and the membrane tube was replaced by a non-porous stainless steel tube.

At steady state, samples at the exit of both the retentate and permeate sides were analyzed by on-line gas chromatography (CE Instruments GC8000). The gas phase separation selectivities (not to be confused with reaction selectivity, which is defined below) were calculated as the ratio of permeances, using the log-mean partial pressure difference in the calculations. For the pervaporation results separation factors were calculated using Eq. (1), where $x_{i\text{-}C_8}$ is the molar fraction of *i*-octene and $x_i$ are the molar fractions of *n*-dodecene or *n*-hexadecene in the retentate; $y_i$ values represent the equivalent molar fractions in the permeate side.

$$\alpha_{C_8/i} = \frac{y_{i\text{-}C_8}/y_i}{x_{i\text{-}C_8}/x_i} \quad (1)$$

In reaction experiments, *i*-butene conversion ($X_{i\text{-butene}}$) was calculated as follows (Eq. (2)).

$$X_{i\text{-butene}} = \frac{\sum_i \nu_i m_{OUT,i} - 4m_{OUT,i\text{-butene}}}{\sum_i \nu_i m_{OUT,i}} \times 100 \quad (2)$$

where $\nu_i$ designates the carbon number of the corresponding species, $m_{OUT,i}$ the total molar flowrate of any compound at the reactor exit (i.e. taking into account retentate + permeate) and $m_{OUT,i\text{-butene}}$ the total molar flowrate of *i*-butene. The reaction selectivity to $C_8$ (calculated as the sum of both 2,4,4-trimethyl-1-pentene and 2,4,4-trimethyl-2-pentene

isomers) and $C_{12}$ (again considering the $C_{12}$ isomers together) was calculated by

$$S_i = \frac{\nu_i m_{\mathrm{OUT},i}}{\sum_i \nu_i m_{\mathrm{OUT},i}} \times 100 \quad (3)$$

where $i \neq i$-butene.

The yields of $i$-butene to $C_8$ and $C_{12}$ can thus be calculated as the product of the $i$-butene conversion by the corresponding reaction selectivity divided by 100. A by-pass stream was analyzed in order to determine accurately the concentration of the feed. Mass balance closures for the different species based in the composition and flowrate of the feed and one (FBR) or two exit streams of the reactor (ZMR) were in the $100 \pm 5\%$ interval.

### 2.1. Reactor simulation

A simplified simulation model was used to assess the improvement that could be expected in this system with the use of the ZMR. Six different reaction schemes were considered and used to fit the experimental data obtained in a FBR. Of these, the kinetic scheme shown in Table 1 was selected, based on the goodness-of-fit attained. This scheme considers the formation of $i$-octene to be proportional to the squared $i$-$C_4$ concentration, while the formation of higher molecular weight products from $i$-octene and $i$-$C_4$ is directly proportional to the concentrations of each of these species. The kinetic parameters are given in Table 1, with their standard errors.

A pseudo-homogeneous plug flow model has been used for the simulation of the FBR and the ZMR. Several simplifying assumptions were made: negligible radial concentration profiles, negligible inter- and intra-particle mass transfer resistance in the catalysts, negligible pressure drop in the catalyst bed and isothermal reactor. The direct contribution of the zeolite membrane to the reaction was neglected, which is reasonable in view of the small mass of zeolite present and the temperatures used in this work. Relatively simple models have been previously used to model the behavior of membrane reactors [14,15], and in spite of their simplicity they were able to predict correctly the experimentally observed reactor behavior. In this case, the permeation rate of the different species was considered proportional to the partial pressure gradient between both sides of the membrane, with a treatment similar to that given by Gokhale et al. [16]. Under these assumptions, at steady-state the mass conservation equation for a given species $i$ results

$$\frac{\mathrm{d}m_i}{\mathrm{d}z} = R_i \rho_L \pi r^2 - 2\pi r \mathrm{PF}_i \quad (4)$$

where $m_i$ is the molar flowrate of component $i$ at a position $z$ in the reactor (mol $s^{-1}$) and $PF_i$ the permeation flux for (mol $m^{-2}$ s). In a FBR the permeation term becomes null for all the species.

Fig. 1 shows the experimental results and the model predictions for the data obtained in a FBR. As can be seen, the agreement is satisfactory, and the simulation model, with the kinetic parameters of Table 1, is capable of predicting the product distribution at the FBR exit. The model was then used to assess the improvement that could be obtained in a ZMR with respect to the FBR. In an ideal ZMR, $i$-octene would block the zeolite channels to the other components, whose permeance would then become null. This has been simulated and the results are shown in Fig. 2 as a reaction selectivity–conversion plot for both reactors. As expected, the reaction selectivity obtained in the ZMR is higher, since the selectively permeated $i$-octene does not react further, and the difference between FBR and ZMR selectivity increases with conversion. However, it is interesting to note that the model predicts not only a higher reaction selectivity for the ZMR, but also a higher conversion for the same nominal value of space time, as seen by comparing the position of points A, B and C for both reactors. This can be explained by taking into account the fact that the selective permeation of $i$-octene increases both the residence time of $i$-butene and its concentration at any axial position in the ZMR compared to the FBR.

Table 1
Reaction scheme and kinetic coefficients selected, with their standard errors[a]

| Reaction scheme | Kinetic equation | $k_i$ (mol $kg^{-1}$ s) |
|---|---|---|
| $i$-$C_4 \rightarrow i$-$C_8$ | $k_1 X_{i\text{-}C_4}^2$ | $0.1066 \pm 0.0033$ |
| $i$-$C_4 \rightarrow i$-$C_{12+}$ | $k_2 X_{i\text{-}C_4}$ | $0.0512 \pm 0.0017$ |
| $i$-$C_8 \rightarrow i$-$C_{12+}$ | $k_3 X_{i\text{-}C_8}$ | $0.0075 \pm 0.0011$ |

[a] $C_{12+}$ represents the sum of concentrations of $C_{12}$ and $C_{16}$ products.

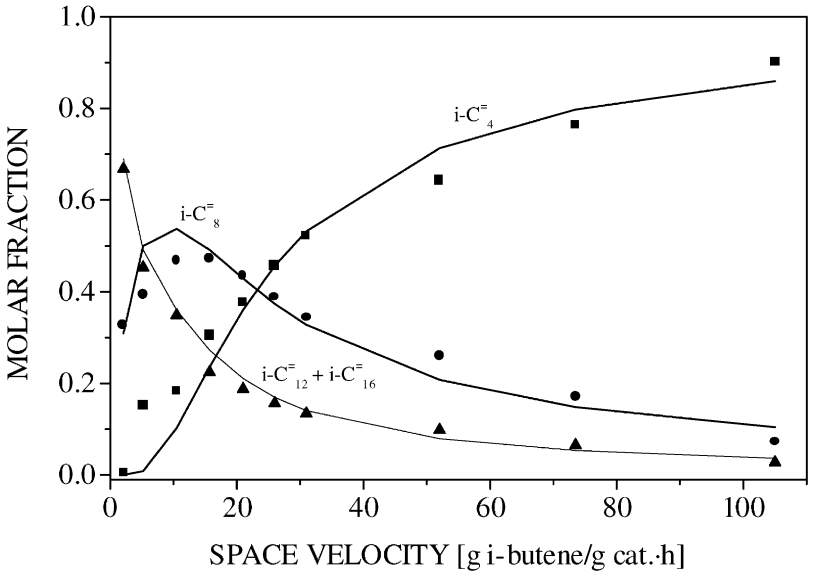


Fig. 1. Comparison between model predictions and experimental results. Molar fractions of the different species at the FBR exit as a function of space time (pressure: 15 bar, temperature: 20°C).

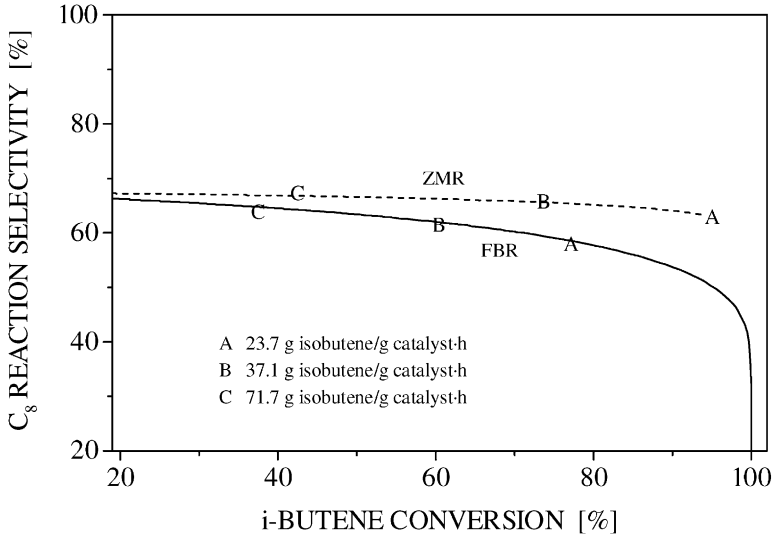


Fig. 2. Simulation results. $C_8$ reaction selectivity vs. *i*-butene conversion for FBR and ZMR. $T = 20°C$, $P = 15$ bar, 0.34 g of catalyst, variable flowrate. A, B and C are simulated points for ZMR and FBR at the same nominal value of the space velocity.

## 3. Experimental results and discussion

Table 2 shows some important characteristics of the silicalite membranes employed in this work. It can be seen that the $N_2$ permeances are in the 1.3–6.6 × $10^{-7}$ mol m$^{-2}$ s$^{-1}$ Pa$^{-1}$ range, and the $N_2/SF_6$ ideal selectivities (ratio of single gas permeances) in the 13–36 range. All these values are in agreement with those previously reported for the preparation of silicalite tubular membranes by secondary growth [11].

Table 2
Some characteristics of the silicalite membranes used in this work

| Membrane | Secondary growth gel | $N_2$ permeanc (mol $m^{-2}$ $s^{-1}$ $Pa^{-1}$) | $N_2/SF_6$ ideal selectivity |
|---|---|---|---|
| M1 | A | $5.5 \times 10^{-7}$ | 16 |
| M2 | B | $3.3 \times 10^{-7}$ | 15 |
| M3 | B | $1.3 \times 10^{-7}$ | 10 |
| M4 | B | $2.2 \times 10^{-7}$ | 13 |

### *3.1. Separation experiments*

#### *3.1.1. Gas phase separation of the 2,4,4-trimethyl-1-pentene/i-butene binary mixture*

Before the reaction experiments, some of the silicalite membranes were tested for the gas phase separation of the 2,4,4-trimethyl-1-pentene/*i*-butene binary mixture. Fig. 3 shows the permeances of 2,4,4-trimethyl-1-pentene and *i*-butene in the binary mixture, as a function of temperature through membrane M1. It can be seen that below 70°C, the permeation of *i*-octene is considerably higher than that of *i*-butene, even though *i*-octene is a molecule with a larger kinetic diameter and thus with a smaller diffusivity. In this case, the separation can be explained as a consequence of the stronger interaction between the longer branched olefin and the zeolitic membrane pores. The preferential adsorption of *i*-octene blocks the access of *i*-butene to the zeolite pores, especially at low temperatures. As the temperature increases adsorption becomes less important and the differences in diffusivity prevail. Another contributing factor may be capillary condensation, since the *i*-butene feed was saturated at room temperature with *i*-octene. Capillary condensation of *i*-octene would be expected to block small inter-crystalline defects, thereby increasing the selectivity, although this contribution would also decrease as the temperature increases. As a consequence of both trends, at temperatures above 70°C *i*-butene permeates faster as can be seen in Fig. 3.

Fig. 4 shows the effect of increasing the feed pressure from 1 atm to approximately 1.9 bar, while keeping the permeate side at atmospheric pressure. Both the *i*-octene and *i*-butene permeances increased

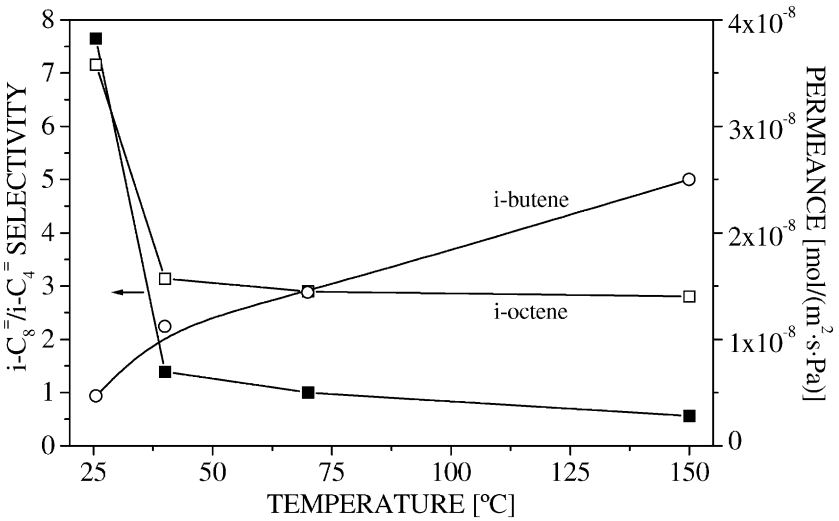


Fig. 3. Gas phase separation results. Permanences of *i*-octene and *i*-butene, and separation selectivity in the binary mixture as a function of temperature. Membrane M1, feed: 25 Nml $min^{-1}$; *i*-octene/*i*-butene molar ratio in the feed: 2.3/97.7 kPa; $N_2$ sweep gas at atmospheric pressure: 9 Nml $min^{-1}$.

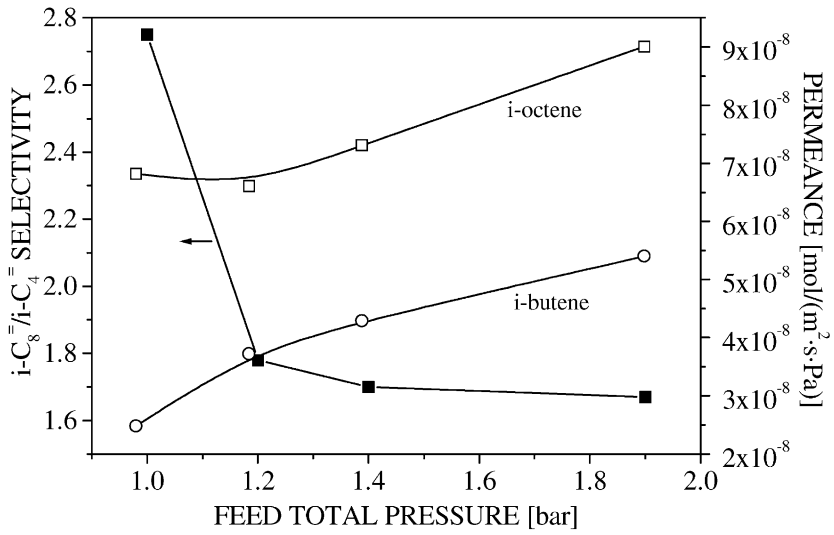


Fig. 4. Gas phase separation results. Permanences of *i*-octene and *i*-butene and separation selectivity in the binary mixture as a function of the total pressure on the feed side. Membrane M4, temperature: 25°C; feed: 25 Nml $min^{-1}$; *i*-octene/*i*-butene molar ratio in the feed: 1.5/98.5; $N_2$ sweep gas at atmospheric pressure: 9 Nml $min^{-1}$.

with pressure, while the *i*-octene/*i*-butene separation selectivity decreased continuously. This can justified considering, non selective transport through inter-crystalline defects increases with pressure; the non-selective transport affects the permeation of *i*-octene and of *i*-butene in a similar way, therefore reducing the separation selectivity.

### *3.1.2. Pervaporation experiments with a ternary mixture containing 2,4,4-trimethyl-1-pentene, 1-dodece and 1-hexadecene*

The ability of the membrane to separate *i*-octene from its higher molecular weight competitors (docedene, $C_{12}$ and hexadecene, $C_{16}$) was tested in liquid-phase pervaporation experiments. Fig. 5 shows the results obtained with membrane M2 as a function of pressure. The same phenomenon is observed (i.e. the lighter component is favored with increasing pressure difference). However, the change in the separation factors is considerably smaller than that observed for the gas phase. This is due to the fact that, for these large molecules, the magnitude of the permeation flux through small intercrystalline defects (viscous flow in the liquid-phase, Knudsen + viscous flow in the gas phase) is less important with liquid-phase mixtures.

In the gas phase experiments with *i*-butene/*i*-octene mixtures, it was shown that, due to preferential adsorption and perhaps also to capillary condensation, the larger molecule was able to block the passage of the smaller one through the zeolite pores. With a further increase in the molecule length (to docedene, $C_{12}$ or hexadecene, $C_{16}$), the relative increase in adsorption strength is smaller. This means that the separation selectivity will mainly be determined by differences in diffusivity, and as a consequence *i*-octene would be expected to permeate faster than dodecene or hexadecene, in agreement with the experimental results of Fig. 5.

## *3.2. Reaction experiments*

### *3.2.1. Comparison of ZMR and FBR: influence of the operating conditions*

Once the ability of the silicalite membranes to separate *i*-$C_8$ from the other species in the reactor ($C_4$, $C_{12}$ and $C_{16}$ hydrocarbons) had been demonstrated in the separation tests, a series of reaction experiments was undertaken to validate the model predictions regarding the superior performance of the ZMR in terms of both conversion and reaction selectivity.

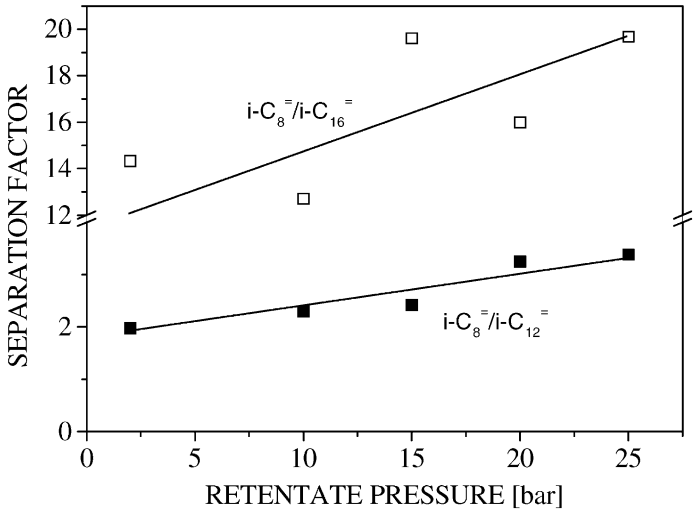


Fig. 5. Liquid-phase separation results. The *i*-octene/1-dodecene and *i*-octene/1-hexadecene separation factors as a function of the retentate pressure. Membrane M2, temperature: 25°C; feed: 0.02–0.47 ml $min^{-1}$; *i*-octene/1-dodecene/1-hexadecene in the feed: 0.25/0.31/0.44; $N_2$ sweep gas at atmospheric pressure: 43 Nml $min^{-1}$.

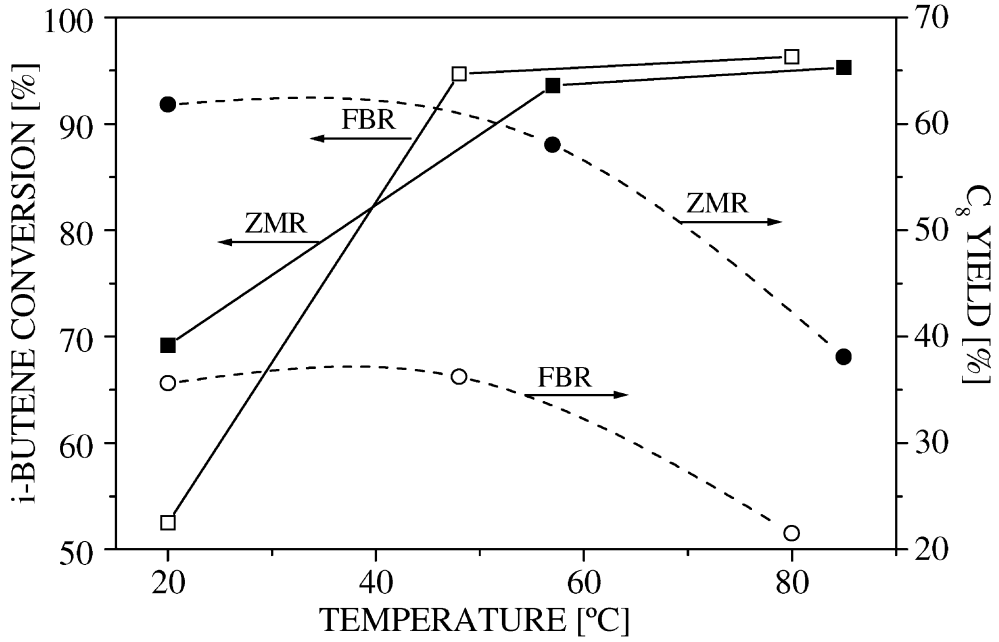


Fig. 6. Comparison of ZMR (membrane M1) and FBR performances. The *i*-butene conversion and *i*-octene yield as a function of temperature. Space velocity: 53g i-butene.g $catalyst^{-1}.h^{-1}$; tube side pressure: 15 bar; $N_2$ sweep gas at atmospheric pressure (ZMR): 1500 Nml $min^{-1}$.

The *i*-butene conversion and the yield to *i*-octene obtained in liquid-phase reaction experiments as a function of temperature are presented in Fig. 6, while the selectivity to the different reaction products is seen in Fig. 7 In this case, 0.35 g of resin mixed with 0.9 g of quartz were loaded inside membrane M1 (ZMR) and inside a stainless steel impervious tube (FBR), so that the space velocity in both reactors was 53g i-butene. g catalyst$^{-1}$.h$^{-1}$.As expected, the *i*-butene conversion increases with temperature in both reactors but, in agreement with the model predictions, at low temperature the conversion is considerably higher (ca. 17% points) in the ZMR. At higher temperatures the conversion is, within experimental error, the same in both reactors. This can be explained as a consequence of two factors: on the one hand, at high temperatures the initial reaction rate is high in both reactors (conversions in the vicinity of 95% are reached), and the increase of residence time that occurs in the ZMR becomes less important. On the other hand, as has been shown, the separation selectivity decreases with temperature, meaning that not only the products, but also the reactants are permeating through the silicalite membrane, with the associated decrease in conversion.

As expected, the conversion increases with temperature, and at the same time the reaction selectivity to the desired product (*i*-$C_8$) consistently decreases in both reactors (Fig. 7), although the values in the ZMR are between 20 and 30% points higher throughout the range investigated. The yield to *i*-$C_8$ (Fig. 6) stays approximately constant below 50°C, where the decrease in reaction selectivity is approximately balanced by the increase in conversion, and decreases thereafter. The largest difference between the ZMR and the FBR takes place at 20°C, where the *i*-octene yields is 26 percentage points higher for the ZMR.

Fig. 8 shows the *i*-butene conversion and the *i*-octene yield obtained with both reactors as a function of the space velocity. The operation temperature was kept constant at 20°C. It can be seen that, while the conversion in both reactors decreases with the space velocity, the decrease in the ZMR is less pronounced, as could be expected since the low temperature employed (20°C) allows the selective permeation of *i*-octene, therefore increasing the residence time of *i*-butene in the reactor. At very low values of the space velocity (high values of the residence time for both reactors) this advantage is lost, and the conversion in the ZMR and FBR is approximately the same. The reaction selectivity plot (Fig. 9) displays a monotonic increase of the *i*-octene selectivity for the FBR, which was expected in view of the strong decrease in *i*-butene conversion shown in Fig. 8 (ca. 70 percentage points). In the ZMR the decrease of conversion is of only 30 percentage points in the same space velocity interval, and the reaction selectivity curve goes

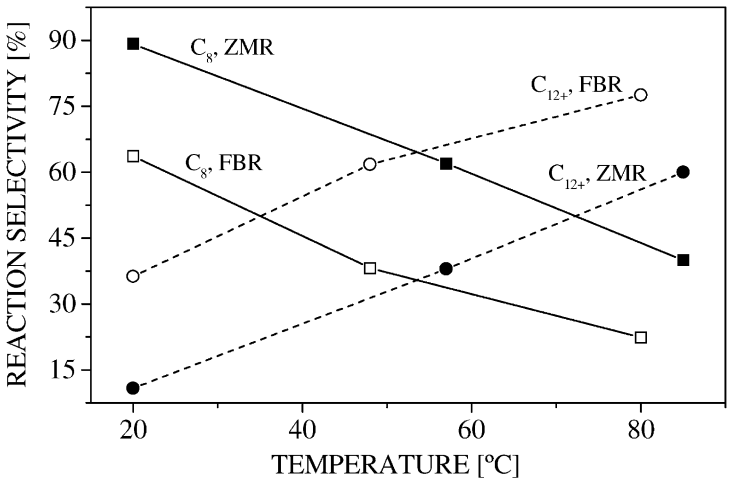


Fig. 7. Comparison of ZMR and FBR performances. The *i*-octene and $C_{12+}$ (*i*-$C_{12}$ + *i*-$C_{16}$) reaction selectivity as a function of temperature. Same conditions as in Fig. 6.

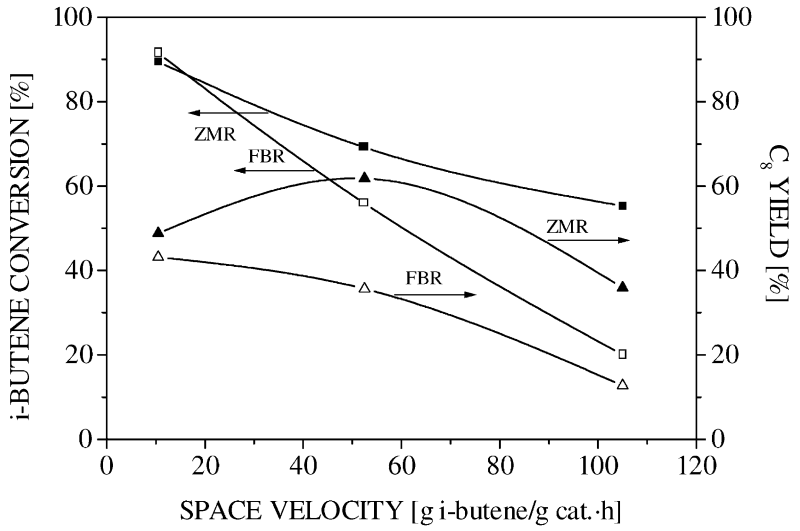


Fig. 8. Comparison of ZMR (membrane M1) and FBR performances. The *i*-butene conversion and *i*-octene yield as a function of the space velocity. Temperature: 20–25°C; tube side pressure: 12–15 bar; $N_2$ sweep gas at atmospheric pressure (ZMR): 1600 Nml $min^{-1}$.

through a maximum. Thus, for moderate increases of the space velocity, the *i*-octene reaction selectivity increases, driven by the decrease in conversion. However, as the space velocity is further increased the time available for permeation of *i*-octene decreases, and a lower reaction selectivity is obtained: at a space velocity of 105 $h^{-1}$, the *i*-octene reaction selectivity in the ZMR and FBR is nearly the same (Fig. 9). Note, however, that the benefits of the ZMR have not been lost, since the same value of *i*-octene reaction selectivity is obtained at an *i*-butene conversion level which is almost three times higher in the ZMR.

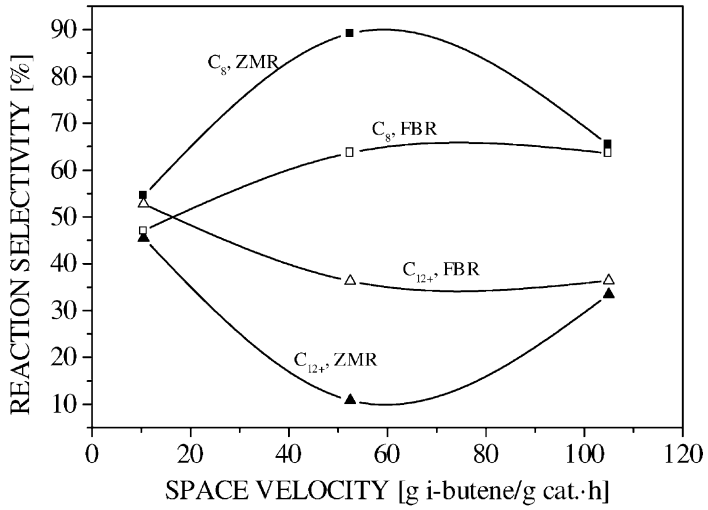


Fig. 9. Comparison of ZMR and FBR performances. The *i*-octene and $C_{12+}$ ($i$-$C_{12} + i$-$C_{16}$) reaction selectivities as a function of the space velocity. Same conditions as in Fig. 8.

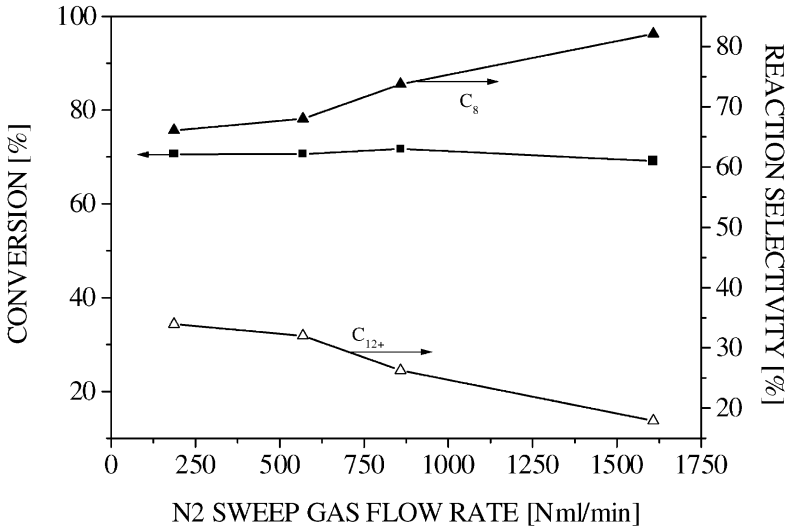


Fig. 10. ZMR results. The *i*-butene conversion and *i*-octene and $C_{12+}$ reaction selectivities as a function of the sweep gas flowrate at atmospheric pressure. Membrane M3, space velocity: 21 $h^{-1}$; temperature: 20°C; tube side pressure: 12 bar.

Finally, Fig. 10 illustrates the effect of the $N_2$ sweep gas in a ZMR. Increasing the flowrate of the sweep gas increases the driving force for permeation (i.e. the partial pressure gradient of all permeating species) between both membrane sides. However, at the low temperature of the experiment (20°C), the zeolite pores and inter-crystalline voids are mainly occupied by *i*-octene, and the increase in the sweep gas flowrate produces a steady increase in the *i*-octene reaction selectivity, which reaches values above 80%.

## 4. Conclusions

Silicalite membranes prepared by secondary growth on stainless steel porous tubes separated selectively *i*-octene from *i*-butene and from $C_{12}$ and $C_{16}$ hydrocarbons under the reaction conditions used for *i*-butene dimerization. The removal of *i*-octene from the reaction environment prevents its further reaction to give undesired $C_{12}$ and $C_{16}$ compounds, and also increases the residence time of the reactants. As a consequence, both *i*-butene conversion and *i*-octene reaction selectivity increased considerably in the ZMR with respect to a conventional FBR. A simplified reactor model using empirically determined reaction kinetics was able to reproduce the main trends observed experimentally. These results indicate that membrane reactors with permeation of reaction products are useful not only to increase conversion in equilibrium-limited reactions, but also to improve the reaction selectivity in consecutive reaction schemes with an intermediate valuable product, provided that this product can be selectively separated at the reaction conditions.

## Acknowledgements

Financial support from DGICYT (QUI97-1085) and DGA (P94/97) is gratefully acknowledged.

## References

[1] J. Coronas, M. Menéndez, J. Santamaría, Chem. Eng. Sci. 49 (1994) 2014.
[2] C. Téllez, M. Menéndez, J. Santamaría, AIChE J. 43 (1997) 777.
[3] M.J. Alfonso, A. Julbe, D. Farruseng, M. Menéndez, J. Santamaría, Chem. Eng. Sci. 54 (1999) 1265.
[4] C. Lange, S. Storck, B. Tesche, W.F. Maier, J. Catal. 175 (1998) 280.
[5] J. Coronas, J. Santamaría, Sep. Pur. Meth. 28 (1999) 127.
[6] D. Casanave, A. Giroir-Fendler, J. Sánchez, R. Louaty, J.A. Dalmon, Catal. Today 25 (1995) 309.
[7] J. van de Graaf, M. Zwiep, F. Kapteijn, J.A. Moulijn, Appl. Catal. A 178 (1999) 225.

[8] M.A. Salomón, J. Coronas, M. Menéndez, J. Santamaría, Appl. Catal. A 200 (2000) 201.
[9] R. Espinoza, E. Du Toit, J. Santamaría, M. Menéndez, J. Coronas, S. Irusta, Stud. Surf. Sci. Catal. 130 (2000) 389.
[10] G. Parkinson, Chem. Eng. 106 (6) (1999) 49.
[11] M. Arruebo, J. Coronas, M. Menéndez, J. Santamaría, Separation of hydrocarbons from natural gas using silicalite membranes, Sep. Pur. Technol., in press.
[12] M.C. Lovallo, M. Tsapatsis, AIChE J. 42 (1996) 3020.
[13] M.D. Jia, B. Chen, R.D. Noble, J.L. Falconer, J. Membrane Sci. 90 (1994) 1.
[14] J. Coronas, A. Gonzalo, D. Lafarga, M. Menéndez, AIChE J. 43 (1997) 3095.
[15] C. Téllez, M. Menéndez, J. Santamaría, Chem. Eng. Sci. 54 (1999) 2917.
[16] Y.V. Gokhale, R.D. Noble, J.L. Falcomer, J. Membrane Sci. 103 (1995) 235.